Binding of Anti-GRP78 Autoantibodies to Cell Surface GRP78 Increases Tissue Factor Procoagulant Activity via the Release of Calcium from Endoplasmic Reticulum Stores*[S]

Ali A. Al-Hashimi[‡], Jennifer Caldwell[‡], Mario Gonzalez-Gronow[§], Salvatore V. Pizzo[§], Danya Aboumrad[‡], Lindsay Pozza[‡], Hiam Al-Bayati[‡], Jeffrey I. Weitz[§¶], Alan Stafford[¶], Howard Chan[¶], Anil Kapoor[‖], Donald W. Jacobsen[**‡‡3], Jeffrey G. Dickhout[§1], and Richard C. Austin[‡¶2]

From the [‡]Department of Medicine and Division of Nephrology and the [‖]Department of Surgery and Division of Urology, St Joseph's Hospital and McMaster University, Hamilton, Ontario L8N 4A6, Canada, the [¶]Thrombosis and Atherosclerosis Research Institute, Hamilton General Hospital and McMaster University, Hamilton, Ontario L8L 2X2, Canada, the [§]Department of Pathology, Medical Center, Duke University, Durham, North Carolina 27710, the [**]Department of Cell Biology, Lerner Research Institute, Cleveland Clinic, Cleveland, Ohio 44195, and the [‡‡]Department of Molecular Medicine, Cleveland Clinic Lerner College of Medicine, Case Western Reserve University, Cleveland, Ohio 44106

The increased risk of venous thromboembolism in cancer patients has been attributed to enhanced tissue factor (TF) procoagulant activity (PCA) on the surface of cancer cells. Recent studies have shown that TF PCA can be modulated by GRP78, an endoplasmic reticulum (ER)-resident molecular chaperone. In this study, we investigated the role of cell surface GRP78 in modulating TF PCA in several human cancer cell lines. Although both GRP78 and TF are present on the cell surface of cancer cells, there was no evidence of a stable interaction between recombinant human GRP78 and TF, nor was there any effect of exogenously added recombinant GRP78 on cell surface TF PCA. Treatment of cells with the ER stress-inducing agent thapsigargin, an inhibitor of the sarco(endo)plasmic reticulum Ca^{2+} pump that causes Ca^{2+} efflux from ER stores, increased cytosolic $[Ca^{2+}]$ and induced TF PCA. Consistent with these findings, anti-GRP78 autoantibodies that were isolated from the serum of patients with prostate cancer and bind to a specific N-terminal epitope (Leu^{98}–Leu^{115}) on cell surface GRP78, caused a dose-dependent increase in cytosolic $[Ca^{2+}]$ and enhanced TF PCA. The ability to interfere with cell surface GRP78 binding, block phospholipase C activity, sequester ER Ca^{2+}, or prevent plasma membrane phosphatidylserine exposure resulted in a significant decrease in the TF PCA induced by anti-GRP78 autoantibodies. Taken together, these findings provide evidence that engagement of the anti-GRP78 autoantibodies with cell surface GRP78 increases TF PCA through a mechanism that involves the release of Ca^{2+} from ER stores. Furthermore, blocking GRP78 signaling on the surface of cancer cells attenuates TF PCA and has the potential to reduce the risk of cancer-related venous thromboembolism.

Venous thromboembolism and other hypercoagulable states are major contributors to death and disability in cancer patients (1, 2). Although the prothrombotic state of cancer can be influenced by the activation of specific oncogenes (3), current evidence suggests that the major impact involves the enhanced expression and/or procoagulant activity (PCA)[4] of tissue factor (TF) on the surface of cancer cells (4).

TF is a 47-kDa transmembrane glycoprotein, and the major physiological initiator of the coagulation cascade (5). TF is normally expressed on the cell surface in a latent or "encrypted" form (6). Following exposure of cells to a number of pathophysiological agents/conditions, including cytokines (7), endotoxin (8), apoptosis (9, 10), hypoxia (11), and/or changes in intracellular $[Ca^{2+}]$ (12, 13), TF is converted into an active or "de-encrypted" form (14). De-encrypted TF on the cell surface binds circulating factor VIIa, and the resulting complex acts as a catalyst for the conversion of factors IX and X to IXa and Xa, respectively. This triggers thrombin generation leading to the formation of a fibrin clot. It is believed that TF de-encryption provides a mechanism by which cells initiate a rapid hemostatic response without the necessity of transcriptional up-regulation of TF. Some proposed mechanisms for modulating TF PCA include the formation of TF homodimers, the phospholipid microenvironment, including phosphatidylserine (PS) exposure, TF compartmentalization in lipid rafts, endocytosis and

[4] The abbreviations used are: PCA, procoagulant activity; ER, endoplasmic reticulum; GRP78, 78-kDa glucose-regulated protein; PLC, phospholipase C; SPR, surface plasmon resonance; TF, tissue factor; Tg, thapsigargin; Tm, tunicamycin; UPR, unfolded protein response; PS, phosphatidylserine; HBSS, Hanks' balanced salt solution; RU, response units; BAPTA, 1,2-bis(2-aminophenoxy)ethane-N,N,N',N'-tetraacetic acid; IP_3, inositol 1,4,5-trisphosphate.

degradation of the TF-FVIIa complex, and isomerization of the TF disulfide bond by protein disulfide isomerase (15, 16).

Besides its critical role in thrombosis and hemostasis, recent studies indicate that TF also promotes cancer growth and metastasis (17–20). It is well established that enhanced TF expression/PCA correlates with cancer progression, angiogenesis, and a malignant phenotype (21, 22). It is believed that TF modulates cancer growth and metastasis by activating the coagulation system at the cell surface or through coagulation-independent signals. In addition, the release of TF-bearing microvesicles from the surface of tumor cells into the circulation can enhance systemic coagulation (23). Despite the causal role of TF in tumorigenesis, the cellular factors that modulate TF expression/PCA in cancer are poorly understood.

Recent studies have reported that TF expression/PCA can be modulated by GRP78, an endoplasmic reticulum (ER)-resident molecular chaperone that facilitates the correct folding and assembly of newly synthesized proteins (24). Overexpression of ER lumenal GRP78 inhibits TF PCA by protecting cells from changes in intracellular Ca^{2+} levels and/or the generation of reactive oxygen species (24). Furthermore, cell surface expression of GRP78 in cultured endothelial cells negatively regulates TF PCA through a direct GRP78/TF interaction (25). However, antibody-mediated GRP78 inhibition on the cell surface resulted in a significant increase in TF PCA. GRP78 is also highly expressed on the surface of many human cancers (26–31), where it functions as a unique signaling receptor to promote cell proliferation and survival (32). Furthermore, exposure of GRP78 on the surface of cancer cells stimulates the production of anti-GRP78 autoantibodies, high levels of which are correlated with accelerated cancer progression, enhanced metastatic potential, and reduced survival (33). We now report that anti-GRP78 autoantibodies isolated from the serum of patients with prostate cancer bind to GRP78 on the surface of cancer cells and enhance TF PCA. Mechanistically, engagement of the autoantibodies with cell surface GRP78 causes PLC-mediated release of Ca^{2+} from ER stores, thereby increasing cytosolic $[Ca^{2+}]$. The increase in cytosolic $[Ca^{2+}]$ alters plasma membrane asymmetry resulting in enhanced TF PCA. Based on these findings, the engagement of anti-GRP78 autoantibodies with cell surface GRP78 may explain how TF is activated on cancer cells and contributes to the hypercoagulable state observed in cancer patients.

EXPERIMENTAL PROCEDURES

Cell Culture—Cancer cell lines were purchased from the American Tissue Culture Collection (Manassas, VA). The human bladder carcinoma cell line T24/83 was cultured in M199 media (Invitrogen), whereas the prostate cancer cell line PC-3 was cultured in F-12 media (Invitrogen). All media was supplemented with 10% fetal bovine serum (Sigma-Aldrich) containing 100 units/ml penicillin and 100 μg/ml streptomycin (Invitrogen). Cells were maintained at 37 °C in a humidified atmosphere of 5% CO_2/95% air.

Production and Purification of Recombinant Human GRP78 in Bacteria—High level expression of recombinant human GRP78 was achieved in bacteria (see supplemental Fig. S1). Briefly, transformed Rosetta (DE3) cells containing the GRP78-

pET-28b construct were grown at 16 °C in LB media and treated with isopropyl β-D-1-thiogalactopyranoside to induce GRP78 expression. GRP78 protein was purified by using a nickel affinity fast protein liquid chromatography (FPLC) system, as described previously (34). Integrity and purity of the recombinant GRP78 protein was assessed by SDS-PAGE (supplemental Fig. S1*A*) and immunoblotting using anti-KDEL antibodies (supplemental Fig. S1*B*). Approximately 5.0 mg of FPLC-purified GRP78 protein was obtained from 400 ml of bacterial culture. Consistent with previous findings for recombinant hamster GRP78 (35), recombinant human GRP78 containing the His tag was functionally active, based on its ATPase (supplemental Fig. S1*C*) and chaperone activities (supplemental Fig. S1*D*).

Patient Samples—Blood samples were obtained from patients with prostate cancer from the Department of Urology, St. Joseph's Healthcare, Hamilton, Ontario, Canada. Written informed consent was obtained from patients and approved by the Research Ethics Board of St. Joseph's Healthcare (REB#08-3047).

Isolation of Anti-GRP78 Autoantibodies—Anti-GRP78 autoantibodies (GRP78 a-AB) were purified from the serum of prostate cancer patients by affinity chromatography on protein A-Sepharose, as previously described (36).

Cell Treatments—Ionomycin (Sigma-Aldrich) and thapsigargin (Tg, Sigma-Aldrich) stock solutions were diluted in DMSO as a transitional solvent and given in the appropriate physiological buffer to achieve a final concentration of 0.5–20 μM. Tg was used as an ER stress inducer and a positive control for the TF PCA assay. Tunicamycin (Tm, Sigma-Aldrich) stocks were diluted in DMSO, and final concentration in physiological buffers ranged from 1 to 10 μg/ml. Tm was used as an inducer of ER stress and a negative control for the TF PCA assay. Phospholipase C (PLC) inhibitor, U73123, and its nonactive analogue, U73122, were obtained from Santa Cruz Biotechnology (Santa Cruz, CA). Both chemicals were diluted to a final concentration of 5–10 μM in 1× TBS. The CNVKSDKSC peptide (GeneMed Synthesis, San Antonio, TX) was resuspended at a concentration of 60 μg/ml in 1× PBS and used to neutralize GRP78 a-AB.

Biotinylation of Cell Surface Proteins—Biotinylation of cell surface proteins was performed using the Cell Surface Protein Isolation Kit (Pierce). Briefly, four T75 flasks of T24/83 cells were grown to 95% confluency, washed twice with ice-cold 1× PBS and incubated in 0.25 mg/ml EZ-Link Sulfo-NHS-SS-Biotin for 30 min at 4 °C with rocking. Following saturation with quenching solution, the cells were scraped, pelleted at 500 × *g* for 3 min, and washed several times with 1× TBS. Cells were lysed in 500 μl of lysis buffer for 30 min on ice with vortexing every 5 min. The lysates were centrifuged at 10,000 × *g* for 2 min at 4 °C, and the biotinylated proteins were isolated from the cleared supernatant by binding to immobilized NeutrAvidin slurry for 60 min at room temperature with rotation. The slurry was washed four times with wash buffer containing protease inhibitors, and the biotinylated proteins were solubilized in 400 μl of 4× SDS-PAGE sample buffer (50 mM Tris, pH 6.8, 2% SDS, 10% glycerol, 0.01% bromphenol blue, and 50 mM DTT) for 60 min at room temperature with rotation. As a control, total cell

lysates were collected in SDS-PAGE sample buffer. Immuno-blot analysis was used to identify target proteins of interest in both total and cell surface lysates.

Immunoblotting—Total cell lysates in 4× SDS-PAGE sample buffer were separated on a 10% SDS-PAGE gel under reducing conditions and transferred to nitrocellulose membranes (Bio-Rad) using the Trans-Blot Semi-Dry transfer apparatus (Bio-Rad). Membranes were blocked overnight in 5% skim milk in 1× TBST and then incubated with a primary antibody (anti-GRP78/Bip, catalog no. 610979, BD Transduction, San Jose, CA; anti-Phospho-eIF2α, catalog no. 9721S, Cell Signaling, Danvers, MA) followed by the appropriate horseradish peroxidase (HRP)-conjugated secondary antibodies (Dako, Carpinteria, CA) diluted in 1× TBST containing 1% skim milk. Membranes were visualized using the Western Lighting Chemiluminescence Reagent (PerkinElmer Life Sciences), and Kodak X-OMAT Blue XB-1 film (PerkinElmer Life Sciences) was exposed and developed using a Kodak X-OMAT 1000A processor. To control for equivalent protein loading, immuno-blots were re-probed with a mouse monoclonal anti-β-actin antibody (catalog no. A5441, Sigma-Aldrich).

FACS Analysis—FACS analysis was used to detect cell surface TF and GRP78. Briefly, non-permeabilized T24/83 cells were detached from cell culture plates using 2 mM EDTA and centrifuged at 200 × g for 5 min at 4 °C. The cell pellet was resuspended in FACS wash buffer (1× PBS/1% FBS) and centrifuged at 200 × g for 3 min. To examine cell surface GRP78, cells were incubated (1:200 dilution) in the presence of anti-GRP78 monoclonal antibodies conjugated to Alexa488 (catalog no. SPA-827-488, Assay Design, Ann Arbor, MI). To examine surface TF, cells were incubated (1:100 dilution) in the presence of a rabbit anti-human TF antibody (catalog no. 4502, American Diagnostica, Stamford, CT) in FACS wash buffer for 40 min on ice. Cells were washed three times with FACS wash buffer and incubated (1:200) with the corresponding secondary antibody (catalog no. A21206, Alexa Fluor 488-conjugated donkey anti-rabbit, Molecular Probes, Carlsbad, CA) in FACS wash buffer for 30 min on ice in the dark. Cells were washed, fixed, and stored in 1% fresh formaldehyde. FACS data analysis was performed using the Cytomics FC 500 Series Flow Cytometry Systems (Beckman Coulter Canada, Mississauga, Ontario, Canada).

Indirect Immunofluorescence—T24/83 cells grown on coverslips were washed with Hanks' balanced salt solution (HBSS) (Invitrogen) containing 1 mM CaCl$_2$, 1 mM MgCl$_2$, and fixed for 30 min at room temperature in 4% fresh formaldehyde in 1× PBS. The slides were then incubated in 5% nonfat milk in 1× PBS for 90 min at room temperature. Excess blocking buffer was removed from the slide, and cells were incubated with a primary sheep anti-GRP78 antibody, goat anti-human tissue factor (catalog no. 4501, American Diagnostica), or a combination of the two in 1% nonfat milk in 1× PBS overnight at 4 °C. The cells were then washed three times in 1× PBST and incubated with a secondary antibody containing a 1:1000 dilution of an Alexa Fluor 568-conjugated donkey anti-sheep IgG, an Alexa Fluor 488-conjugated rabbit anti-goat IgG, or a mixture of the two for 90 min at 4 °C in the dark. As controls, cells were incubated with the secondary IgG alone. Finally, the cells

were washed three times with 1× PBS and mounted. Images were captured using a Zeiss Axio Observer fluorescence microscope equipped with a 100×/1.4 numerical aperture Plan Apochromat oil immersion lens (Carl Zeiss, Thornwood, NY). Confocal data were collected as previously described (37), and optical sections were three-dimensionally reconstructed using an average intensity algorithm for projections of optical section stacks using ImageJ version 1.37 (National Institutes of Health, Bethesda, MD).

SPR—Potential biomolecular interactions were investigated using a Biacore 1000 biosensor system (Biacore, Amersham Biosciences). Biotinylated recombinant human GRP78 or ovalbumin, diluted in filtered and degassed Hepes-buffered saline (20 mM Hepes, 150 mM NaCl, pH 7.4) containing 2 mM CaCl$_2$ and 0.005% Tween 20 (HBS-Tw), was adsorbed to a Biacore streptavidin SA chip at a flow rate of 5 μl/min at 25 °C until 1300 response units (RU) of biotinylated GRP78 or 2500 RU of ovalbumin were adsorbed. To determine the binding of recombinant human TF (a generous gift from Dr. George P. Vlasuk, Corvas Pharmaceuticals) to GRP78, 30-μl aliquots, in concentrations ranging from 62.5 to 2000 nM, were injected over the flow cell**s** at a flow rate of 10 μl/min for ~5 min, followed by a 5-min wash to monitor association and dissociation, respectively. It was not necessary to regenerate the flow cells between the injections. As a positive control, an anti-human GRP78 polyclonal antibody (catalog no. C20, Santa Cruz Biotechnology) was injected over the flow cells at a concentration of 4 μg/ml using the same protocol. Peak RU values determined for each recombinant TF concentration were corrected for the RU values with control ovalbumin.

Continuous Measurement of Cell Surface TF PCA—We have recently developed a continuous assay for the measurement of TF PCA on intact cancer cells (31). Briefly, cells were seeded into a 96-well tissue culture plate (1 × 10^4 cells/well) the day before the experiment. The culture media was then removed, and the cells were washed once with 1× TBS. A mixture containing 1 nM human FVIIa, 30 nM human FX, 10 mM CaCl$_2$, and 0.4 mM chromogenic substrate S-2765 (Diapharma, West Chester, OH) in 1× TBS was added to each well. Following addition of the test agent diluted in 1× TBS, the absorbance at 405 nm was measured every 2 min for 3 h at 37 °C. A standard curve was generated where 100 units of TF activity was defined as the amount of activity in 0.3 μl of human recombinant TF, which is equivalent to 450 μg of TF (as determined by the American Diagnostica ELISA). V_{max} was calculated using Soft-Max Pro and used to determine the amount of FXa generated per 10,000 cells (units/10,000 cells).

RNA Isolation and RT-PCR—RNA was isolated using an RNeasy Mini kit (Qiagen), and cDNA was synthesized using a High Capacity cDNA Reverse Transcription kit (Applied Biosystems). Real-time RT-PCR reactions were carried out based on protocols described previously using SYBR Green MasterMix (Applied Biosystems) (38, 39) using primers listed in Table 1.

Calcium Imaging—Confluent cells (1 × 10^4 cells per well) grown in 96-well plates were washed in HBSS (Invitrogen) containing 20 mM HEPES. Fura-2 AM was prepared in 20% pluronic acid F127 (Invitrogen) in DMSO. A 10 μM working solu-

TABLE 1
Quantitative RT-PCR primers

Gene	Forward primer	Reverse primer
Spliced *XBP1*	5′–TTGAGAACCAGGAGTTAAG–3′	5′–CTGCACCTGCTGCGGACT–3′
CHOP	5′–AGAACCAGGAAACGGAAACAGA–3′	5′–TCTCCTTCATGCGCTGCTTT–3′
β-ACTIN	5′–TGGGCATGGGTCAGAAGGAT–3′	5′–AAGCATTTGCGGTGGACGAT–3′

tion of Fura 2-AM in HBSS was incubated on the cells at room temperature for 30 min. Cells were washed three times with HBSS and preincubated in HBSS for 15 min before experiments at 37 °C to allow for de-esterification of the dye. Plates were read at 37 °C kinetically at two wavelengths (λ), λ_1 (340 nm excitation, 515 nm emission, measuring dye bound to Ca^{2+}), and λ_2 (380 nm excitation, 515 nm emission, measuring unbound dye). Measurements were made for 5 min to establish a baseline followed by the addition of the agonist Tg (1 μM), Tm (5 μg/ml), or ionomycin (10 μM) diluted in 1× PBS. PBS was also used without test substance as a vehicle control. Plates were then read kinetically at λ_1 and λ_2 for 30 min to establish a ratio of Ca^{2+} bound over free dye representing the change in cytosolic [Ca^{2+}].

Measurement of Intracellular Calcium in Single Cells—Intracellular calcium in T24/83 cells was measured using the fluorescent indicator Fura-2 AM (40). The cells were plated on sterile coverslips in 35-mm tissue culture dishes and incubated at 37 °C for 18–24 h. On the day of the experiment, Fura-2 AM (2 mM) was added, and the dish was incubated at 37 °C for 30 min. Cell monolayers were then rinsed twice with HBSS containing 10 mM HEPES, pH 7.4, 3.5 mM NaHCO$_3$, and once with DMEM containing 0.1% BSA. Cell monolayers grown on coverslips were placed on the inverted microscope stage, and intracellular [Ca^{2+}] was measured using a Digital Imaging Microscopy system (Inovision Corp., Research Triangle Park, NC) employing dual excitation ratio imaging techniques at 37 °C. After collecting baseline data, increasing concentrations of the anti-GRP78 autoantibodies was added to the cell monolayers to determine the effect of ligand binding on calcium mobilization. A digitized video image was obtained by averaging up to 256 frames with the following filter combination: Fura-2 excitation, 340 and 380 nm; emission, >450 nm. Routinely, excitation intensity was attenuated 100- to 1000-fold before reaching the cell, and the background images were obtained. Intracellular [Ca^{2+}] was measured by subtracting the background from images on a pixel basis. To obtain the intracellular [Ca^{2+}] for an individual cell, the mean value of the pixel ratio for the cell was compared with values obtained with the same equipment using Fura-2-containing EGTA-Ca^{2+} buffers (41).

Statistical Analysis—Excel software was used to determine the standard error of the mean for each treatment. Significance of differences between control and various treatments was determined by analysis of variance. On finding significance with analysis of variance, an unpaired Student's *t* test was performed. For all analyses, $p \leq 0.05$ was considered significant.

RESULTS

T24/83 Cells Express Cell Surface GRP78 and TF—We (24, 31) as well as others (42) have demonstrated that the T24/83 human bladder carcinoma cell line displays prothrombotic characteristics due to enhanced TF expression and PCA. Based on these findings, T24/83 cells were chosen as our cancer cell model to investigate the effect of cell surface GRP78 on TF PCA.

A number of studies have identified GRP78 on the surface of a variety of human cancer cells (26–31, 43–45). To determine if GRP78 is similarly expressed on the surface of T24/83 cells, cell surface proteins were isolated using a biotin-based technique followed by immunoblotting with anti-GRP78 antibodies. GRP78 was identified in both total cell lysates and on the cell surface of T24/83 cells using this approach (Fig. 1*A*). As expected, TF was predominantly expressed on the cell surface, consistent with its localization in the plasma membrane. In contrast to GRP78 and TF, several nuclear proteins, including proliferating cell nuclear antigen and lamin B were exclusively found in the total cell lysates and not on the cell surface. Consistent with these biochemical findings, FACS analysis (Fig. 1*B*) and three-dimensional image reconstruction of optical sections captured using confocal microscopy (Fig. 1*C*) demonstrated the presence of GRP78 on the cell surface. In these reconstructions, GRP78 was observed throughout the cell surface; however, punctuate regions of high GRP78 expression were apparent above the nucleus. Indirect immunofluorescence on non-permeabilized cells showed the presence of GRP78 and TF on the surface of T24/83 cells (Fig. 1*D*). Both cell surface GRP78 and TF were expressed in a similar staining pattern over the cell surface. Negative controls with the secondary antibody alone showed little or no immunofluorescence. Taken together, these findings demonstrate that T24/83 cells actively express both GRP78 and TF on their cell surface.

GRP78 Does Not Directly Bind to TF or Modulate TF PCA—Previous studies have suggested that GRP78 can negatively regulate procoagulant activity by directly associating with TF on the cell surface of endothelial cells (25). Although anti-GRP78 antibodies were able to immunoprecipitate TF, as observed on immunoblots, anti-TF antibodies failed to pull down GRP78 (data not shown). To further assess the direct interaction between GRP78 and TF, surface plasmon resonance (SPR) was used to measure binding between immobilized recombinant human GRP78 and full-length non-lipidated recombinant human TF. As shown in Fig. 2*A* (*upper panel*), the shallow and linear slope of the dose-response curves between TF and GRP78 suggests no specific binding. As a positive control, a strong and direct interaction was observed between the immobilized GRP78 and an anti-GRP78 antibody (Fig. 2*A*, *bottom panel*). Further, treatment of quiescent T24/83 cells with increasing doses of recombinant GRP78 had no effect on TF PCA (Fig. 2*B*). Because exogenous recombinant GRP78 did not activate TF PCA on quiescent T24/83 cells, we examined whether it could modulate TF PCA induced by thapsigargin. Again, increasing doses of recombinant GRP78 had no effect on
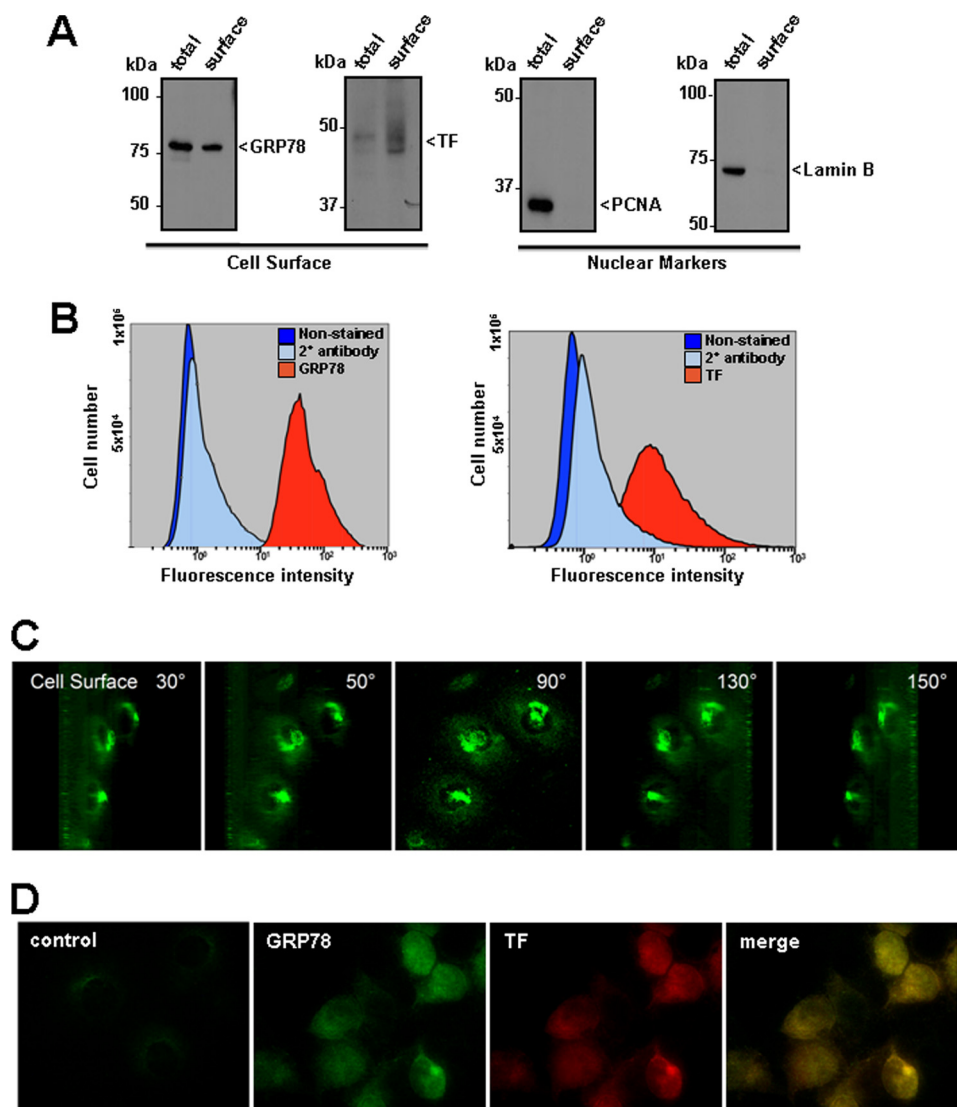
FIGURE 1. GRP78 and TF are expressed on the surface of T24/83 cells. *A*, cell surface proteins were biotinylated, and cell lysates were subjected to streptavidin pulldown. Cell surface proteins were eluted, separated on 10% SDS-PAGE gels, transferred to nitrocellulose membranes, and immunoblotted with antibodies to GRP78 (*GRP78*), anti-proliferating nuclear cell antigen (*PCNA*), lamin B (*lamin B*), or TF (*TF*). Cell surface fractions (*surface*) were compared with proteins in total cell lysates (*total*). The nuclear markers PCNA and Lamin B are not present in the surface fractions. *B*, cell surface GRP78 and TF were detected by FACS analysis using antibodies against GRP78 or TF, respectively. Secondary antibody staining alone and unstained cells acted as negative controls. *Histograms* were generated using the Cytomics FC 500 series flow cytometry software. *C*, T24/83 cells grown on coverslips were fixed without permeabilization, immunostained for GRP78, and subjected to confocal analysis. Optical sections of the cells were three-dimensionally reconstructed and projected using ImageJ software at rotation angles of 30, 50, 90, 130, and 150 degrees to visualize cell surface GRP78. *D*, identification of cell surface GRP78 and TF in T24/83 cells. Co-immunostaining for GRP78 and TF was performed on fixed, non-permeabilized cells and viewed by fluorescence microscopy. Regions of cell surface overlap for GRP78 and TF in the *merged image* appear as *yellow* staining.

ferase activity and *N*-linked glycosylation (46) without altering cytosolic $[Ca^{2+}]$. Immunoblotting showed that both thapsigargin and tunicamycin caused ER stress and unfolded protein response (UPR) induction, as measured by a temporal increase in eIF2α phosphorylation and GRP78 protein levels (Fig. 3*A*). Further, quantitative RT-PCR demonstrated a similar increase in the mRNA levels for CHOP as well as the spliced form of XBP-1 in T24/83 cells treated with thapsigargin or tunicamycin (Fig. 3*B*). However, only thapsigargin was able to increase cytosolic $[Ca^{2+}]$ (Fig. 3*C*). As expected, ionomycin treatment also caused a significant and sustained increase in cytosolic $[Ca^{2+}]$. Comparison of the effect of tunicamycin and thapsigargin on TF PCA revealed that only thapsigargin dose-dependently increased TF PCA in T24/83 cells (Fig. 3*D*). Given that thapsigargin depletes ER Ca^{2+} stores and increases cytosolic $[Ca^{2+}]$, we investigated whether chelating the free cytosolic Ca^{2+} would reduce TF PCA activation. Pretreatment of cells with 1,2-bis(2-aminophenoxy)ethane-*N,N,N′,N′*-tetraacetic acid (BAPTA), a specific Ca^{2+} chelator (47), significantly reduced thapsigargin-mediated TF PCA (Fig. 3*E*). These findings suggest that increases in cytosolic $[Ca^{2+}]$ induce TF PCA independent of ER stress and UPR activation.

Anti-GRP78 Autoantibodies Increase Cytosolic $[Ca^{2+}]$ and Induce TF PCA—Previous studies have reported that anti-GRP78 autoantibodies from prostate cancer patients bind to cell surface GRP78 on several human prostate cancer cell lines and cause the release of Ca^{2+} from ER stores (26). Consistent with these findings, anti-GRP78 autoantibodies were able to dose-dependently increase cytosolic $[Ca^{2+}]$ over a human IgG control in T24/83 cells (Fig. 4*A*). Importantly, autoantibody concentrations of 60 μg/ml caused a >6-fold increase in cytosolic $[Ca^{2+}]$, intracellular levels that are necessary to up-regulate TF PCA (15). To elucidate the effect of anti-GRP78 autoantibodies on TF PCA, cells were treated with 7 increasing concentrations of the anti-GRP78 autoantibody: 7 μg/ml, which corresponds to the maximum levels observed in the healthy population, and 30–60 μg/ml, which corresponds to the levels observed in prostate

the ability of thapsigargin to enhance TF PCA (Fig. 2*C*). These findings suggest that GRP78 does not directly bind to TF and fails to modulate TF PCA on T24/83 cells.

Increased Cytosolic $[Ca^{2+}]$ and Not UPR Activation Induces TF PCA in T24/83 Cells—We have demonstrated recently that the ER stress-inducing agents ionomycin and thapsigargin up-regulate TF PCA by increasing cytosolic $[Ca^{2+}]$ (24, 31). To determine whether increased TF PCA results from UPR activation or a specific elevation of cytosolic $[Ca^{2+}]$ brought about by thapsigargin, T24/83 cells were also treated with tunicamycin, an inducer of ER stress that inhibits GlcNAc phosphotrans-
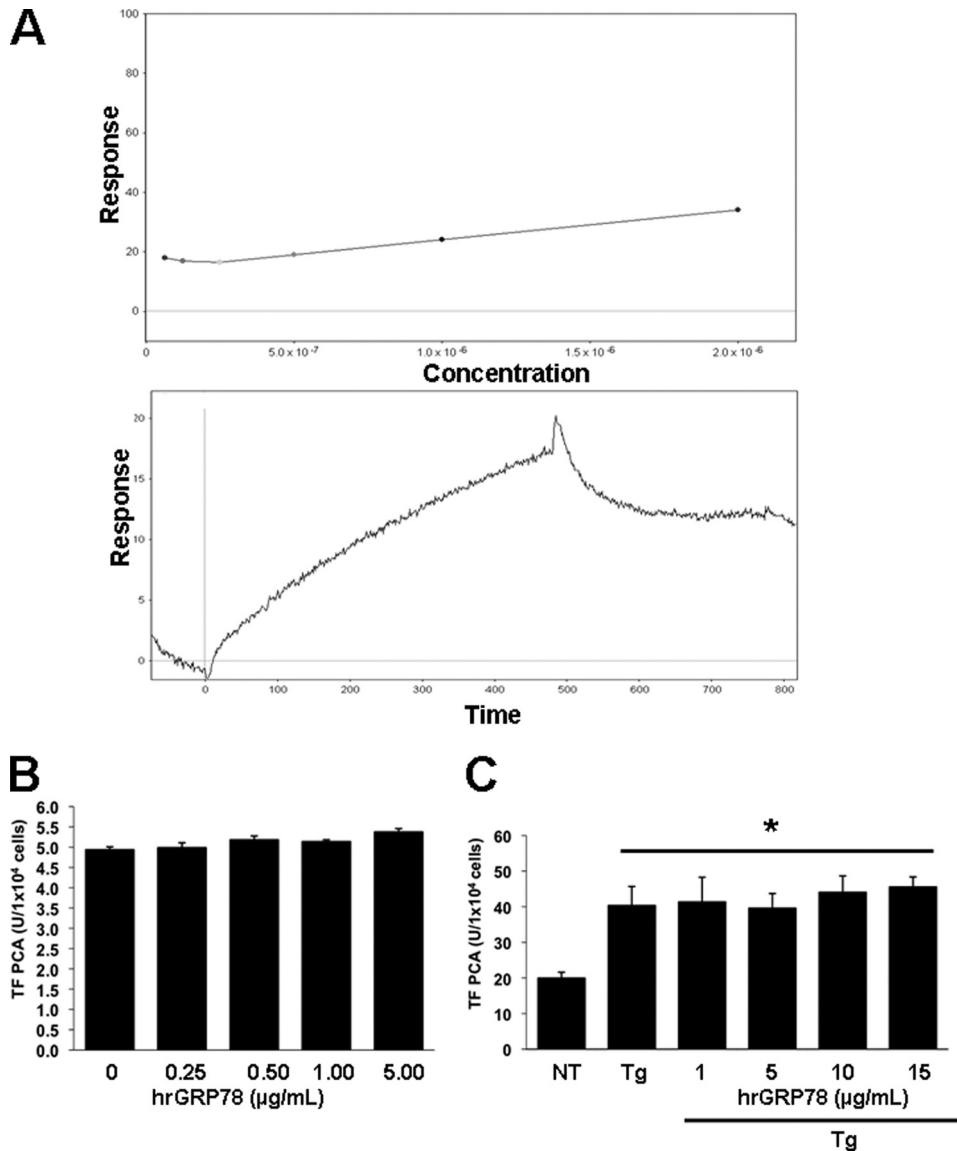
FIGURE 2. **Recombinant human GRP78 does not bind to TF and fails to modulate TF PCA.** *A*, binding of recombinant human GRP78 to TF using SPR. Biotinylated recombinant human GRP78 was adsorbed to a separate flow cell of an SA BIAcore chip containing pre-immobilized streptavidin to ~1300 RU. As a control, ovalbumin was adsorbed to a separate flow cell to ~2500 RU. Increasing concentrations of recombinant human TF (62.5–2000 nM) were injected into the flow cells at 10 μl/min, followed by a 5-min wash to monitor dissociation (*top panel*). Data indicate that the addition of increasing doses of TF do not bind to immobilized GRP78. As a positive control, robust binding was demonstrated between an anti-GRP78 antibody and the immobilized GRP78. *B*, effect of exogenous recombinant human GRP78 on TF PCA. T24/83 cells (1 × 10⁴ cells/well) seeded in a 96-well plate were treated with increasing doses of exogenous recombinant human GRP78 (*hrGRP78*) for 3 h, and TF PCA was measured using the continuous assay (*n* = 8). *C*, effect of exogenous recombinant human GRP78 (*hrGRP78*) on TF PCA induced by thapsigargin. T24/83 cells were seeded in a 96-well plate and treated with 5 μM thapsigargin (*Tg*) in the absence or presence of increasing concentrations of exogenous recombinant human GRP78. TF PCA was measured using the continuous assay (*n* = 8). *, *p* < 0.05 *versus* non-treated cells (*NT*).

cancer patients (Fig. 4*B*) (26). Our results demonstrated that treatment of cells with 7 μg/ml of the anti-GRP78 autoantibodies had no effect on TF PCA. However, 60 μg/ml of the autoantibody caused a significant increase in TF PCA similar to that observed with thapsigargin (Fig. 4*B*). A similar enhancement in TF PCA was observed with 30 μg/ml of the autoantibody. This effect on TF PCA was abolished by preincubation with an anti-TF inhibitory antibody, implying that this effect was mediated exclusively by TF. In contrast, the nonspecific anti-GFP antibody had no significant effect on TF PCA induced by the

autoantibodies. To further confirm the role of cell surface GRP78 in TF PCA following treatment with the anti-GRP78 autoantibodies, we utilized the prostate cancer cell line (PC-3) that expresses TF (31) but low levels of cell surface GRP78 (Fig. 4*C*) (26). Both T24/83 and PC-3 cells were treated with thapsigargin or anti-GRP78 autoantibodies, and TF PCA was measured (Fig. 4*D*). Thapsigargin treatment elicited a significant up-regulation of TF PCA for both cell lines. In contrast, autoantibody treatment up-regulated TF PCA in the T24/83 but not PC-3 cells, suggesting that cell surface GRP78 is necessary for autoantibody-mediated TF PCA.

Pretreatment with the CNVKS-DKSC Peptide Blocks Autoantibody-mediated TF PCA in T24/83 Cells—Anti-GRP78 autoantibodies produced by prostate cancer patients bind to a peptide containing the primary amino acid sequence CNVKSDKSC, which mimics the linear primary amino acid sequence Leu⁹⁸–Leu¹¹⁵ located in the N-terminal region of GRP78 (33). Based on these findings, we determined whether the CNVKSDKSC peptide inhibits TF PCA in T24/83 cells treated with the anti-GRP78 autoantibodies. As shown in Fig. 5*A*, pretreatment of the anti-GRP78 autoantibodies with the CNVKS-DKSC peptide significantly inhibited TF PCA in T24/83 cells. The observation that the CNVKSDKSC peptide failed to inhibit TF PCA following thapsigargin treatment indicates that the peptide has no direct inhibitory effect on TF PCA (data not shown).

Anti-GRP78 Autoantibody Increases Cytosolic [Ca²⁺] via Phospholipase C Activation—It has been reported that cell surface GRP78 interacts with a heterotrimeric G protein, resulting in Gqα-protein-dependent activation of phospholipase C (PLC) (48). PLC cleaves phosphatidylinositol 4,5-bisphosphate to produce diacylglycerol and IP₃. Once formed, IP₃ molecules bind specific IP₃ receptors/Ca²⁺ channels on the ER membrane (49), thereby increasing cytosolic [Ca²⁺], which could enhance TF PCA. To evaluate the role of PLC in autoantibody-mediated TF PCA, T24/83 cells were treated with the PLC inhibitor U73122 or its non-active analogue U73343. As shown in Fig. 5*B*, treatment of cells with
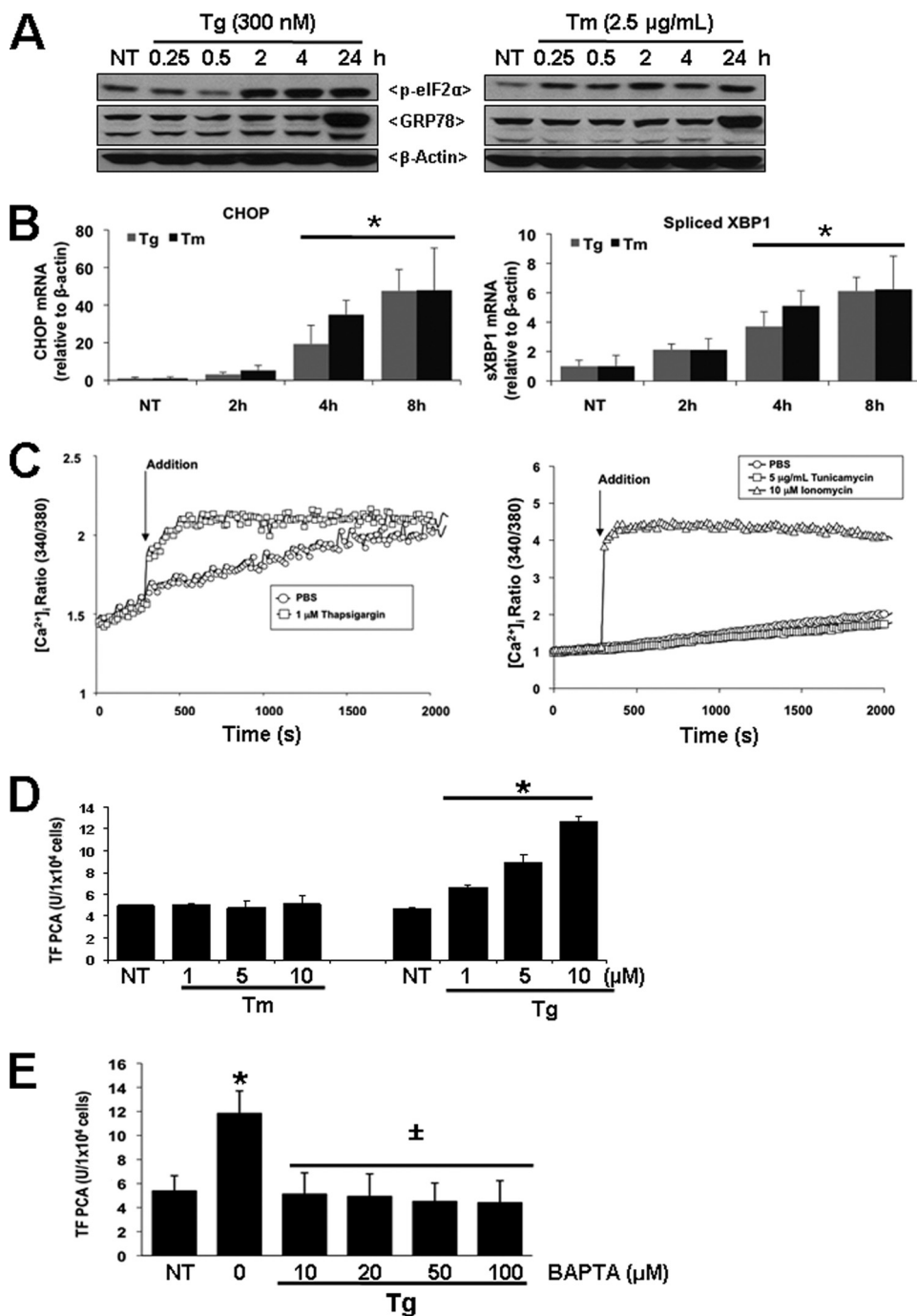
FIGURE 3. **Differential effects of ER stress agents on cytosolic [Ca²⁺] and TF PCA in T24/83 cells.** *A*, detection of UPR markers in T24/83 cells following treatment with tunicamcyn (*Tm*) or thapsigargin (*Tg*). T24/83 cells in 6-well plates were treated with ER stress-inducers tunicamycin (2.5 μg/ml) or thapsigargin (300 nM) for 24 h. Total protein lysates solubilized in SDS-PAGE sample buffer were separated in 10% SDS-PAGE gels, transferred to nitrocellulose membranes, and immunoblotted for phospho-eIF2α (*p-eIF2α*) and GRP78. Membranes were stripped and reprobed with β-actin as a loading control. Results shown are representative of three independent experiments. *B*, quantitative RT-PCR analysis of CHOP and spliced XBP-1 mRNA in T24/83 cells treated with thapsigargin or tunicamycin for 2, 4, and 8 h. Total RNA was isolated, reverse transcribed to single-stranded cDNA, and analyzed by quantitative RT-PCR using primers specific for human CHOP or spliced XBP1. Results are expressed as -fold induction of target gene mRNA levels *versus* β-actin. *, $p < 0.05$ *versus* non-treated (*NT*) cells. *C*, effect of thapsigargin or tunicamycin on cytosolic [Ca²⁺] in T24/83 cells. Calcium fluorometry of T24/83 cells treated with thapsigargin (1 μM), tunicamycin (5 μg/ml), ionomycin (10 μM), or drug vehicle (1× PBS), was determined utilizing the ratiometric calcium-sensitive dye Fura-2 AM. Ratiometric measurements were made for 30 min after agonist stimulation. *D*, TF PCA in T24/83 cells following treatment with increasing concentrations of thapsigargin or tunicamycin. *, $p < 0.01$ *versus* non-treated cells (*NT*). *E*, TF PCA in T24/83 cells following treatment with 5 μM thapsigargin (positive control). T24/83 cells were pre-treated for 30 min in the absence or presence of increasing doses of BAPTA. *, $p < 0.05$ *versus* non-treated cells (*NT*). $^{\pm}$, $p < 0.05$ *versus* Tg-treated cells.

U73122, but not U73343, dose-dependently inhibited the up-regulation of TF PCA induced by the anti-GRP78 autoantibodies.

Tunicamycin Pretreatment Reduces TF PCA—GRP78 is a major ER lumenal Ca²⁺-storage protein, and its overexpression can protect cells from Ca²⁺-induced cytotoxicity (50). Preconditioning of cells with sub-lethal doses of tunicamycin can increase GRP78 protein levels and prevent disturbances in ER Ca²⁺ (51). Based on these findings, T24/83 cells were pretreated with tunicamycin for 24 h to induce the expression of GRP78 (Fig. 3*A*) without an up-regulation of TF PCA (Fig. 3*C*). Following tunicamycin pretreatment, T24/83 cells were tested for TF PCA up-regulation in the absence or presence of either thapsigargin or anti-GRP78 autoantibodies. As shown in Fig. 5*C*, tunicamycin pretreatment significantly reduced the effects of thapsigargin or anti-GRP78 autoantibodies on TF PCA. Furthermore, tunicamycin pretreatment caused a significant repression in TF PCA in non-treated T24/83 cells.

Annexin V Inhibits TF PCA Mediated by Thapsigargin or Anti-GRP78 Autoantibodies—Increases in cytosolic [Ca²⁺] have been shown to activate TF at the cell surface by perturbing the plasma membrane PS asymmetry leading to exposure of PS molecules (15) and the acceleration of coagulation reactions on the cell surface (16, 52–54). Treatment of T24/83 cells with increasing doses of annexin V, a specific PS-binding protein (16), resulted in a significant repression in TF PCA mediated by thapsigargin or anti-GRP78 autoantibodies (Fig. 5*D*). Unlike tunicamycin pretreatment, annexin V had no inhibitory effect on TF PCA in non-treated T24/83 cells.

DISCUSSION

The majority of tumor cells display increased TF expression and the prothrombotic state observed in cancer patients has been largely attributed to the activation of TF
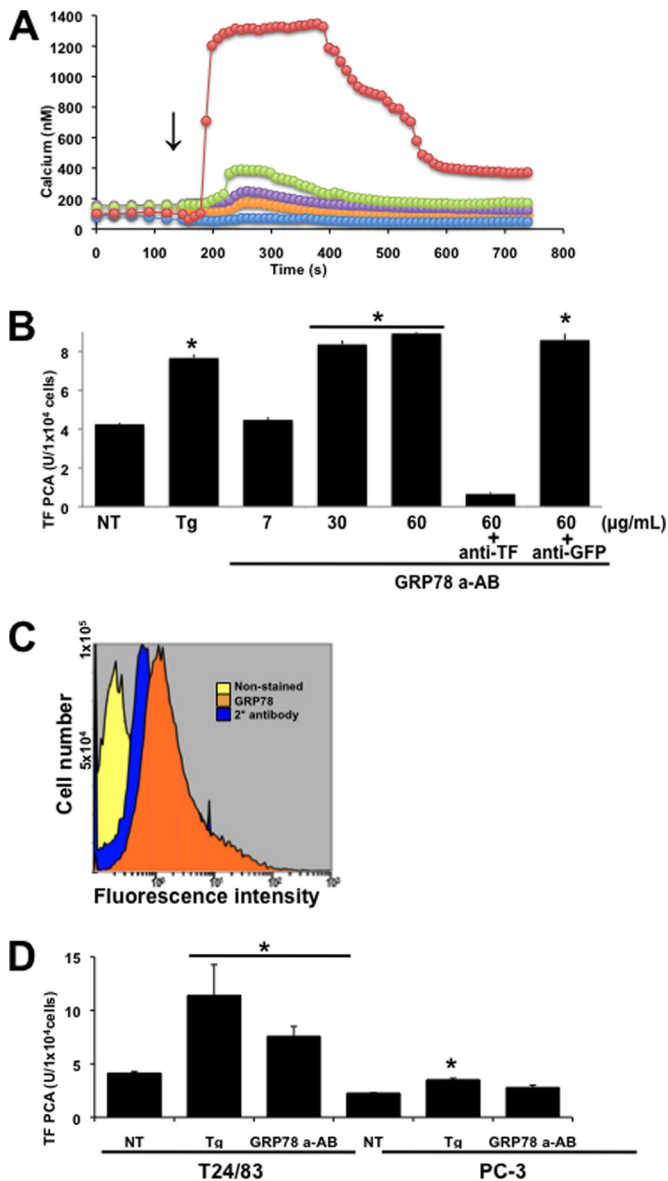
FIGURE 4. **Effect of anti-GRP78 autoantibodies on cytosolic [Ca^{2+}] and TF PCA.** *A*, T24/83 cells were loaded with Fura-2 AM (4 μM), and changes in intracellular [Ca^{2+}] were measured using digital imaging microscopy on single cells after the addition of 5 (*orange circles*), 10 (*violet circles*), 20 (*green circles*), or 60 (*red circles*) μg/ml of anti-GRP78 autoantibodies. Human IgG (*blue circles*) was used as a negative control. *B*, TF-PCA on intact T24/83 cells treated with 5 μM (Tg) thapsigargin or increasing concentrations of the anti-GRP78 autoantibody (*GRP78 a-AB*). *60+antiTF* represents cells pretreated for 1 h with 10 μg/ml of an anti-TF neutralizing antibody. *60+antiGFP* represents cells pretreated for 1 h with 10 μg/ml anti-GFP antibody. TF-PCA was measured continuously for 3 h on T24/83 cells treated with 60 μg/ml of the anti-GRP78 autoantibody (*GRP78 a-AB*). *C*, cell surface detection of GRP78 on PC-3 cells by FACS analysis using antibodies against GRP78. Secondary antibody staining alone and unstained cells acted as negative controls. *Histograms* were generated using the Cytomics FC 500 series flow cytometry software. *D*, TF-PCA was measured in T24/83, and PC-3 cells were treated in the absence or presence of 5 μM thapsigargin (*Tg*) or 60 μg/ml anti-GRP78 autoantibody (*GRP78 a-AB*). *, $p < 0.05$ *versus* non-treated cells (*NT*).

(4). Our previous studies have demonstrated that overexpression of GRP78 in the ER lumen inhibits TF PCA by protecting cells from changes in cytosolic [Ca^{2+}] and/or the generation of reactive oxygen species (24, 37). However, unlike normal cells, GRP78 is present on the cell surface of a wide variety of human cancer cells (26–31, 43–45). In this study, we investigated

whether the presence of cell surface GRP78 modulates TF PCA in T24/83 cells, a well established human bladder carcinoma cell line with prothrombotic characteristics (42). Our findings suggest that the binding of anti-GRP78 autoantibodies to cell surface GRP78 causes PLC-mediated release of Ca^{2+} from ER stores, thereby increasing cytosolic [Ca^{2+}]. This in turn alters plasma membrane asymmetry resulting in enhanced TF PCA. Thus, our findings may explain how TF is activated on the surface of cancer cells and contributes to the hypercoagulable state observed in cancer patients.

Our initial experiments were designed to assess the effects of ER stress-inducing agents on cytosolic [Ca^{2+}] and TF PCA. Treatment of T24/83 cells with thapsigargin or tunicamycin, two well known ER stress-inducing agents, elicited diametrically opposed effects on TF PCA. Thapsigargin, a well defined sarco/endoplasmic reticulum Ca^{2+}-ATPase pump inhibitor, induces ER stress by depleting ER Ca^{2+} stores and increasing cytosolic [Ca^{2+}] (55). In contrast, tunicamycin induces ER stress by inhibiting *N*-linked glycosylation (46). Both tunicamycin and thapsigargin induced ER stress in T24/83 cells, as demonstrated by a similar activation of UPR markers. However, unlike thapsigargin, tunicamycin treatment did not increase cytosolic [Ca^{2+}]. Moreover, thapsigargin, but not tunicamycin treatment, dose-dependently up-regulated TF PCA suggesting that depletion of ER Ca^{2+} stores and not ER stress/UPR activation is required for the up-regulation of TF PCA. Further support for this concept comes from the additional observation that chelation of cytosolic Ca^{2+} with BAPTA-AM attenuated thapsigargin-induced TF PCA.

The ability of tunicamycin to induce the expression of GRP78 without altering cytosolic [Ca^{2+}] implies that pretreatment with this ER stress-inducing agent could potentially inhibit TF PCA. This is based on previous studies showing that GRP78 is a major ER lumenal Ca^{2+}-storage protein and protects from Ca^{2+}-induced cell death (50). In a previous study, we also reported that overexpression of GRP78 by tunicamycin reduces the release of Ca^{2+} from ER stores (37). Indeed, tunicamycin preconditioning inhibited TF PCA induced by anti-GRP78 autoantibodies or thapsigargin. These findings provide evidence that suppressing the release of ER Ca^{2+} by overexpressing GRP78, and likely other ER chaperones in the ER lumen, can block TF PCA.

Cell surface biotinylation was used to demonstrate the expression of TF as well as GRP78 on the surface of T24/83 cells, a finding consistent with other cancer cells (26–30). Indirect immunofluorescence and FACS analysis confirmed the presence of cell surface GRP78 and TF. Three-dimensional reconstructions of optical sections acquired by confocal microscopy revealed high GRP78 expression above the nucleus of T24/83 cells. Although not completely understood, localization of GRP78 expression to this region may reflect distinct focal points for the recruitment of GRP78 to the cell surface. Thus, it is interesting to note that ER-resident chaperone proteins such as GRP78, calnexin, and calreticulin can associate with focal adhesions to mediate IL-1-induced Ca^{2+} signaling (56, 57).

The cellular localization of GRP78 to the ER lumen is dictated by its C-terminal KDEL (Lys-Asp-Glu-Leu) sequence, an ER retention signal found on many ER-resident chaperones (30,
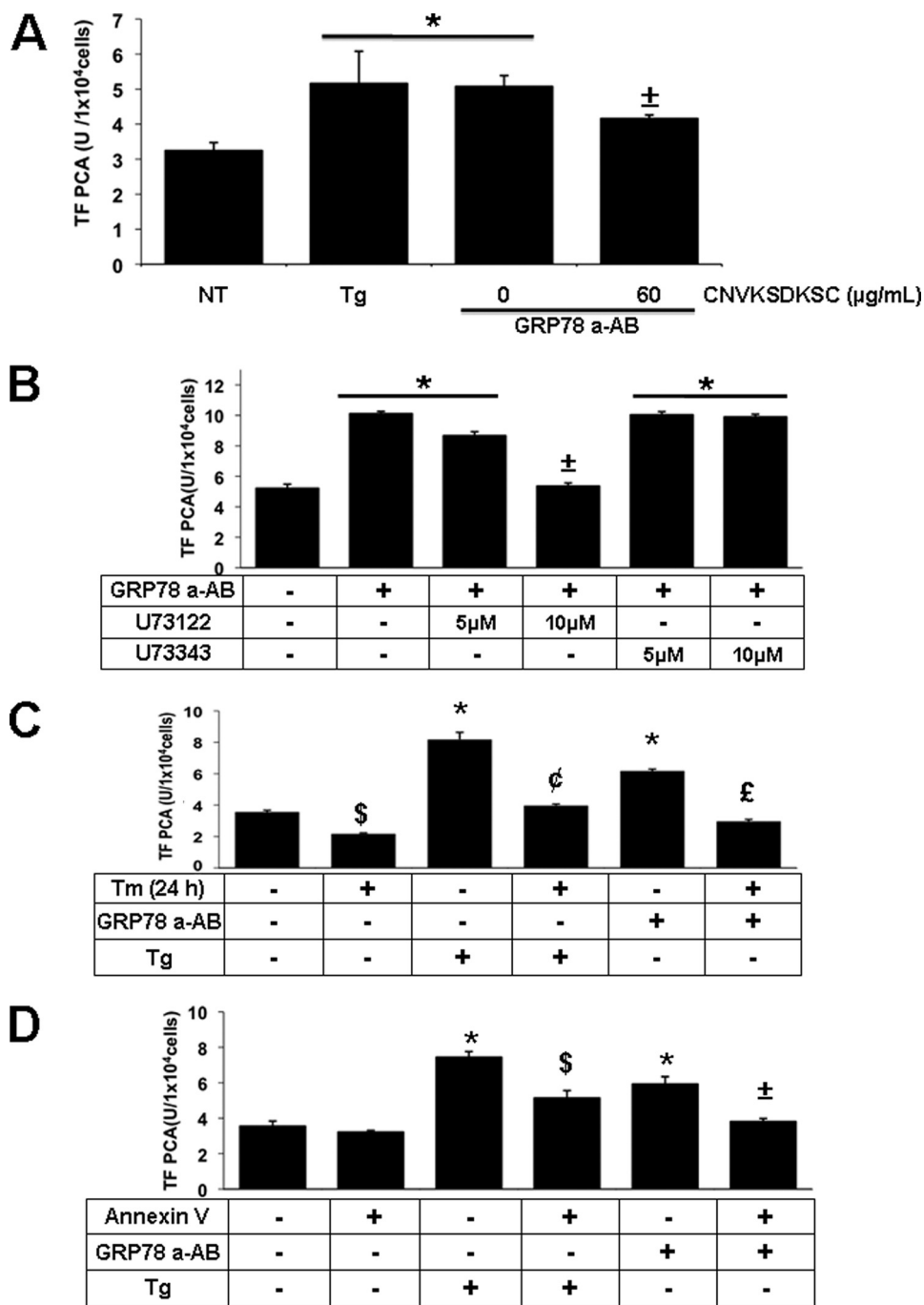
FIGURE 5. **Binding of anti-GRP78 autoantibodies to cell surface GRP78, changes in cytosolic [Ca²⁺] or alterations in plasma membrane integrity modulate TF PCA.** A, effect of CNVKSDKSC peptide on TF PCA induced by anti-GRP78 autoantibodies. TF-PCA was measured on intact T24/83 cells treated with 5 μM thapsigargin (Tg) or 60 μg/ml anti-GRP78 autoantibodies (GRP78 a-AB) in the absence or presence of 60 μg/ml CNVKSDKSC peptide. *, $p < 0.05$ versus non-treated cells (NT). $^{\pm}$, $p < 0.05$ versus cells treated with thapsigargin or the anti-GRP78 autoantibodies. B, effect of PLC inhibition on TF PCA induced by anti-GRP78 autoantibodies. T24/83 cells were pretreated for 1 h in the absence or presence of 5 or 10 μM of the active or non-active PLC inhibitors, U73122 or U73343, respectively. TF-PCA was then measured on intact T24/83 cells treated with 60 μg/ml anti-GRP78 autoantibodies (GRP78 a-AB). *, $p < 0.005$ versus non-treated cells. $^{\pm}$, $p < 0.05$ versus cells treated with U73122 or U73343. C, effect of tunicamycin pre-conditioning on TF PCA induced by 5 μM thapsigargin (Tg) or 60 μg/ml anti-GRP78 autoantibodies. T24/83 cells were grown in the absence or presence of low-dose tunicamycin (Tm, 2.5 μg/ml) for 24 h. Following washing with 1× TBS, cells were placed in fresh growth media for 3 h before the addition of 5 μM thapsigargin (Tg) or 60 μg/ml anti-GRP78 autoantibodies. TF PCA was measured continuously for 3 h following the addition of thapsigargin or anti-GRP78 autoantibodies. *, $p < 0.05$ versus untreated cells (NT). $^{\$}$, $p < 0.05$ versus untreated cells (NT). $^{¢}$, $p < 0.05$ versus thapsigargin treated cells. $^{£}$, $p < 0.05$ versus autoantibody treated cells. D, effect of annexin V pre-treatment on TF PCA. TF PCA was measured continuously for 3 h on intact T24/83 cells treated with 5 μM thapsigargin (Tg) or 60 μg/ml anti-GRP78 autoantibodies (GRP78 a-AB) in the absence or presence of 2.5 μg/ml annexin V (2.5 μg/ml). *, $p < 0.05$ versus non-treated cells (NT). $^{\$}$, $p < 0.05$ versus thapsigargin treated cells. $^{\pm}$, $p < 0.05$ versus autoantibody treated cells.

58, 59). However, GRP78 is found on the cell surface of many cancer cells where it acts as a signaling receptor (26, 29, 32). Currently, it remains unclear how GRP78 escapes ER retrieval mechanisms mediated by the KDEL receptor, given that GRP78 isolated from the cell surface retains its KDEL sequence (30, 58). Two possible explanations are that the KDEL receptors on the ER membrane are down-regulated, modified, or saturated with other ER lumenal proteins or that the KDEL sequence on GRP78 is somehow masked by the co-chaperone MTJ-1 (60). Recent studies have also demonstrated that ER stress may mediate specific mechanisms for GRP78 surface localization and/or ER retention (58). In addition to its cell surface localization on cancer cells, the ability of GRP78 to be incorporated into the plasma membrane is of major interest. Previous studies have demonstrated a subpopulation of GRP78 that is present on the cytosolic surface of the ER membrane (61), consistent with that of a transmembrane protein. In addition to GRP78, calnexin is another ER transmembrane protein found on the cell surface (62).

Recent studies have suggested a direct GRP78/TF interaction at the surface of cultured vascular endothelial cells (25) and platelets (63), suggesting that GRP78 can directly bind TF to negatively regulate its activity (25). However, our SPR studies failed to reveal binding of functional recombinant GRP78 to TF. Although we could immunoprecipitate TF from the surface of T24/83 cells with anti-GRP78 antibodies, in reciprocal experiments we were unable to immunoprecipitate cell surface GRP78 with an anti-TF antibody. These observations suggest in cancer cells that the interaction between cell surface GRP78 and TF is weak or that an antibody-mediated conformational change occurs in cell surface GRP78 or TF that alters binding. The inability of exogenously added human recombinant GRP78 to modulate TF PCA on the sur-
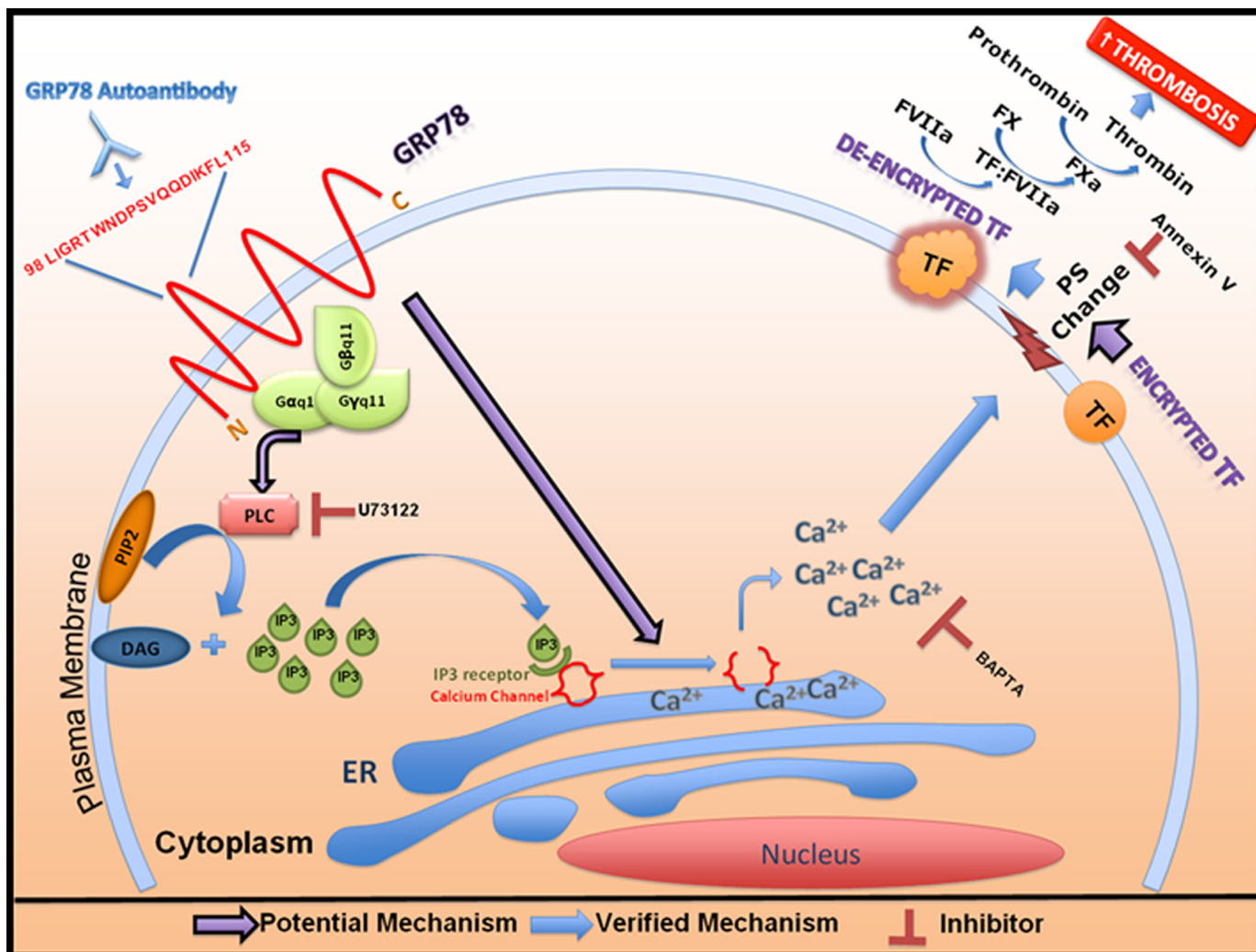
FIGURE 6. **A model for enhanced TF PCA following the binding of anti-GRP78 autoantibodies to cell surface GRP78.** Cell surface GRP78 forms a putative complex with the G-protein-11 (G-α,β,γ-11) complex. Anti-GRP78 autoantibodies bind to the Leu^{98}–Leu^{115} N-terminal domain of GRP78 exposed on the cell surface. Upon binding, a signaling cascade involving Gα_{q11} is activated, leading to enhanced PLC activation and inositol 1,4,5-trisphosphate (IP$_3$) production. IP$_3$ molecules can readily diffuse through the cytosol where they bind to their specific receptors on the ER, leading to the opening of Ca^{2+} channels on the ER membrane and elevating cytosolic [Ca^{2+}]. This increase in cytosolic [Ca^{2+}] can result in TF de-encryption by disrupting plasma membrane asymmetry and leading to the exposure of PS on the cell surface. TF de-encryption triggers an increase in TF PCA, resulting in increased thrombosis.

face of resting or activated T24/83 cells again implies no direct interaction. This finding is consistent with a recent report demonstrating that exogenously added recombinant GRP78 does not bind to the cell surface (58). Although our findings suggest that GRP78 and TF do not form a direct complex, at least in the context of purified components, we cannot rule out the possibility that GRP78 and TF form transient multiprotein complexes on the cell surface, in different cell types or under varying stress conditions, such as ER or oxidative stress. Clearly, additional studies are required to further clarify the cellular factors or stress conditions that affect GRP78/TF interactions on the cell surface.

The topography of cell surface GRP78 and its adaptation to function as a signaling receptor can somehow affect its immunogenicity (26, 32, 33). Autoantibodies to GRP78 have been identified in the serum from patients with prostate, ovarian, or gastric cancer (32, 33). In virtually all these cancers, these autoantibodies recognize the linear GRP78 primary amino acid sequence Leu^{98}–Leu^{115}, implying that this region in the N-ter-

minal domain of cell surface GRP78 is highly immunogenic. In terms of clinical significance, the presence of anti-GRP78 autoantibodies in human plasma correlates with accelerated cancer progression, enhanced metastatic potential, and reduced survival (33). In this study, we showed that treatment of T24/83 cells with levels of anti-GRP78 autoantibodies (60 μg/ml) comparable to those found in the plasma of prostate cancer patients caused a significant increase in cytosolic [Ca^{2+}] and enhanced TF PCA. In contrast, exposure of the cells to lower concentrations of these anti-GRP78 autoantibodies (7 μg/ml) found in the plasmas of healthy individuals failed to affect cytosolic [Ca^{2+}] or up-regulate TF PCA (26). As confirmation for a role of cell surface GRP78 in activating TF PCA, we utilized the PC-3 prostate cancer cell line that expresses TF but little or no GRP78 on the cell surface (26). Here, we were able to show that treatment with anti-GRP78 autoantibodies did not enhance TF PCA; however, a significant increase in TF PCA was still observed when PC-3 cells were treated with thapsigargin. Taken together, these findings suggest that, in addition to

GRP78 exposure on the cell surface, the TF PCA response also requires the presence of a certain threshold level of circulating anti-GRP78 autoantibodies.

The receptor function of cell surface GRP78 has been demonstrated in respect to α_2M signaling (64) and as a co-receptor for the COX A9 virus (65, 66). Additionally, immunoprecipitation studies of plasma membrane fractions from activated α_2M stimulated macrophages demonstrated cell surface GRP78 coupled to the pertussis toxin-insensitive G-protein, $G\alpha_{q11}$ (48). Studies have demonstrated that anti-GRP78 autoantibodies bind to the same tertiary epitope on GRP78 (Leu^{98}–Leu^{115}) as α_2M (26), suggesting that similar signaling mechanisms with anti-GRP78 autoantibodies may be similar to those with α_2M. Treatment with the PLC inhibitor, U73122, but not its non-active analogue, U73343, inhibited TF PCA elicited by the anti-GRP78 autoantibodies. Activation of PLC increases cytosolic inositol 1,4,5-trisphosphate (IP_3), which then binds to specific receptors on ER Ca^{2+} channels and causes ER Ca^{2+} release (49). These results are consistent with a mechanism of increased cytosolic $[Ca^{2+}]$ mediating the effect of GRP78 autoantibodies on TF PCA (Fig. 6), similar to that observed for thapsigargin (31).

The binding of anti-GRP78 autoantibodies to cell surface GRP78 can increase cytosolic $[Ca^{2+}]$ at levels sufficient to disturb flippase activity (15, 16) and therefore may cause exposure of PS molecules on the cell surface. Previous studies have shown that PS expression on the cell surface de-encrypts TF and facilitates its interaction with its co-factor FVIIa (15). Based on our findings, we present a model in Fig. 6 showing that engagement of GRP78 autoantibodies with cell surface GRP78 activates PLC, which triggers an increase in $[IP_3]$ and subsequent ER Ca^{2+} release. This in turn leads to PS exposure, TF de-encryption, and enhanced TF PCA, which culminates in a fibrin-rich clot. In addition to its role in thrombosis, enhanced TF PCA is also linked to increased tumor cell survival, angiogenesis, and metastasis (17–20, 67–69). Thus, strategies aimed at blocking cell surface GRP78 signaling have the potential of decreasing the risk of cancer-related thrombotic events as well as tumor growth.

REFERENCES

1. Sousou, T., and Khorana, A. A. (2009) *Arterioscler. Thromb. Vasc. Biol.* **29,** 316–320
2. Sud, R., and Khorana, A. A. (2009) *Thromb. Res.* **123,** Suppl. 4, S18–S21
3. Boccaccio, C., Sabatino, G., Medico, E., Girolami, F., Follenzi, A., Reato, G., Sottile, A., Naldini, L., and Comoglio, P. M. (2005) *Nature* **434,** 396–400
4. Yu, J. L., May, L., Lhotak, V., Shahrzad, S., Shirasawa, S., Weitz, J. I., Coomber, B. L., Mackman, N., and Rak, J. W. (2005) *Blood* **105,** 1734–1741
5. Mackman, N. (2004) *Arterioscler. Thromb. Vasc. Biol.* **24,** 1015–1022
6. Bach, R. R., and Moldow, C. F. (1997) *Blood* **89,** 3270–3276
7. Conway, E. M., Bach, R., Rosenberg, R. D., and Konigsberg, W. H. (1989) *Thromb. Res.* **53,** 231–241
8. Erlich, J., Fearns, C., Mathison, J., Ulevitch, R. J., and Mackman, N. (1999) *Infect. Immun.* **67,** 2540–2546
9. Bombeli, T., Karsan, A., Tait, J. F., and Harlan, J. M. (1997) *Blood* **89,** 2429–2442
10. Greeno, E. W., Bach, R. R., and Moldow, C. F. (1996) *Lab. Invest.* **75,** 281–289
11. Kobayashi, Y., Yoshimura, N., Nakamura, K., Yamagishi, H., and Oka, T. (1998) *Transplantation* **66,** 708–716
12. Carson, S. D., Perry, G. A., and Pirruccello, S. J. (1994) *Blood* **84,** 526–534
13. Consonni, R., and Bertina, R. M. (1995) *Thromb. Haemost.* **74,** 904–909
14. Bach, R., and Rifkin, D. B. (1990) *Proc. Natl. Acad. Sci. U.S.A.* **87,** 6995–6999
15. Bach, R. R. (2006) *Arterioscler. Thromb. Vasc. Biol.* **26,** 456–461
16. Wolberg, A. S., Monroe, D. M., Roberts, H. R., and Hoffman, M. R. (1999) *Blood Coagul. Fibrinolysis* **10,** 201–210
17. Kasthuri, R. S., Taubman, M. B., and Mackman, N. (2009) *J. Clin Oncol.* **27,** 4834–4838
18. Milsom, C., and Rak, J. (2008) *Pathophysiol. Haemost. Thromb.* **36,** 160–176
19. Rak, J., Milsom, C., Magnus, N., and Yu, J. (2009) *Best Pract. Res. Clin. Haematol.* **22,** 71–83
20. Rak, J., Milsom, C., and Yu, J. (2008) *Curr. Opin. Hematol.* **15,** 522–528
21. Abdulkadir, S. A., Carvalhal, G. F., Kaleem, Z., Kisiel, W., Humphrey, P. A., Catalona, W. J., and Milbrandt, J. (2000) *Hum. Pathol.* **31,** 443–447
22. Kaushal, V., Mukunyadzi, P., Siegel, E. R., Dennis, R. A., Johnson, D. E., and Kohli, M. (2008) *Appl. Immunohistochem. Mol. Morphol.* **16,** 1–6
23. Al-Nedawi, K., Meehan, B., Micallef, J., Lhotak, V., May, L., Guha, A., and Rak, J. (2008) *Nat. Cell. Biol.* **10,** 619–624
24. Watson, L. M., Chan, A. K., Berry, L. R., Li, J., Sood, S. K., Dickhout, J. G., Xu, L., Werstuck, G. H., Bajzar, L., Klamut, H. J., and Austin, R. C. (2003) *J. Biol. Chem.* **278,** 17438–17447
25. Bhattacharjee, G., Ahamed, J., Pedersen, B., El-Sheikh, A., Mackman, N., Ruf, W., Liu, C., and Edgington, T. S. (2005) *Arterioscler. Thromb. Vasc. Biol.* **25,** 1737–1743
26. Gonzalez-Gronow, M., Cuchacovich, M., Llanos, C., Urzua, C., Gawdi, G., and Pizzo, S. V. (2006) *Cancer Res.* **66,** 11424–11431
27. Pozza, L. M., and Austin, R. C. (2005) *Arterioscler. Thromb. Vasc. Biol.* **25,** 1529–1531
28. Shin, B. K., Wang, H., Yim, A. M., Le Naour, F., Brichory, F., Jang, J. H., Zhao, R., Puravs, E., Tra, J., Michael, C. W., Misek, D. E., and Hanash, S. M. (2003) *J. Biol. Chem.* **278,** 7607–7616
29. Misra, U. K., Gonzalez-Gronow, M., Gawdi, G., Hart, J. P., Johnson, C. E., and Pizzo, S. V. (2002) *J. Biol. Chem.* **277,** 42082–42087
30. Xiao, G., Chung, T. F., Pyun, H. Y., Fine, R. E., and Johnson, R. J. (1999) *Brain Res. Mol. Brain Res.* **72,** 121–128
31. Caldwell, J. A., Dickhout, J. G., Al-Hashimi, A. A., and Austin, R. C. (2010) *Lab. Invest.* **90,** 953–962
32. Gonzalez-Gronow, M., Selim, M. A., Papalas, J., and Pizzo, S. V. (2009) *Antioxid Redox Signal* **11,** 2299–2306
33. Mintz, P. J., Kim, J., Do, K. A., Wang, X., Zinner, R. G., Cristofanilli, M., Arap, M. A., Hong, W. K., Troncoso, P., Logothetis, C. J., Pasqualini, R., and Arap, W. (2003) *Nat. Biotechnol.* **21,** 57–63
34. Junop, M. S., Modesti, M., Guarné, A., Ghirlando, R., Gellert, M., and Yang, W. (2000) *EMBO J.* **19,** 5962–5970
35. Wei, J., and Hendershot, L. M. (1995) *J. Biol. Chem.* **270,** 26670–26676
36. Mavropoulos, J. C., Cuchacovich, M., Llanos, C., Aguillón, J. C., Gatica, H., Pizzo, S. V., and Gonzalez-Gronow, M. (2005) *J. Rheumatol.* **32,** 2116–2124
37. Dickhout, J. G., Sood, S. K., and Austin, R. C. (2007) *Antioxid Redox Signal* **9,** 1863–1873
38. Bookout, A. L., and Mangelsdorf, D. J. (2003) *Nucl. Recept. Signal* **1,** e012
39. Bustin, S. A., Benes, V., Garson, J. A., Hellemans, J., Huggett, J., Kubista, M., Mueller, R., Nolan, T., Pfaffl, M. W., Shipley, G. L., Vandesompele, J., and Wittwer, C. T. (2009) *Clin. Chem.* **55,** 611–622
40. Gonzalez-Gronow, M., Gawdi, G., and Pizzo, S. V. (1993) *J. Biol. Chem.* **268,** 20791–20795
41. Grynkiewicz, G., Poenie, M., and Tsien, R. Y. (1985) *J. Biol. Chem.* **260,** 3440–3450
42. López-Pedrera, C., Jardí, M., Inglés-Esteve, J., Muñoz-Cánoves, P., Dorado, G., Velasco, F., and Félez, J. (1997) *Am. J. Hematol.* **56,** 71–78
43. Davidson, D. J., Haskell, C., Majest, S., Kherzai, A., Egan, D. A., Walter, K. A., Schneider, A., Gubbins, E. F., Solomon, L., Chen, Z., Lesniewski, R., and Henkin, J. (2005) *Cancer Res.* **65,** 4663–4672
44. Wiest, D. L., Bhandoola, A., Punt, J., Kreibich, G., McKean, D., and Singer, A. (1997) *Proc. Natl. Acad. Sci. U.S.A.* **94,** 1884–1889

45. Delpino, A., and Castelli, M. (2002) *Biosci. Rep.* **22,** 407–420
46. Price, N. P., and Tsvetanova, B. (2007) *J. Antibiot. (Tokyo)* **60,** 485–491
47. Sergeev, I. N. (2005) *J. Steroid. Biochem. Mol. Biol.* **97,** 145–151
48. Misra, U. K., and Pizzo, S. V. (2008) *J. Cell. Biochem.* **104,** 96–104
49. van Rossum, D. B., and Patterson, R. L. (2009) *Cell. Calcium* **45,** 535–545
50. Lièvremont, J. P., Rizzuto, R., Hendershot, L., and Meldolesi, J. (1997) *J. Biol. Chem.* **272,** 30873–30879
51. Hung, C. C., Ichimura, T., Stevens, J. L., and Bonventre, J. V. (2003) *J. Biol. Chem.* **278,** 29317–29326
52. Zwaal, R. F., and Schroit, A. J. (1997) *Blood* **89,** 1121–1132
53. Kunzelmann-Marche, C., Satta, N., Toti, F., Zhang, Y., Nawroth, P. P., Morrissey, J. H., and Freyssinet, J. M. (2000) *Thromb. Haemost.* **83,** 282–289
54. Lentz, B. R. (2003) *Prog. Lipid Res.* **42,** 423–438
55. Inesi, G., Hua, S., Xu, C., Ma, H., Seth, M., Prasad, A. M., and Sumbilla, C. (2005) *J. Bioenerg. Biomembr.* **37,** 365–368
56. Wang, Q., Rajshankar, D., Branch, D. R., Siminovitch, K. A., Herrera Abreu, M. T., Downey, G. P., and McCulloch, C. A. (2009) *J. Biol. Chem.* **284,** 20763–20772
57. Wang, Q., Herrera Abreu, M. T., Siminovitch, K., Downey, G. P., and McCulloch, C. A. (2006) *J. Biol. Chem.* **281,** 31093–31105
58. Zhang, Y., Liu, R., Ni, M., Gill, P., and Lee, A. S. (2010) *J. Biol. Chem.* **285,** 15065–15075
59. Andres, D. A., Rhodes, J. D., Meisel, R. L., and Dixon, J. E. (1991) *J. Biol. Chem.* **266,** 14277–14282
60. Misra, U. K., Gonzalez-Gronow, M., Gawdi, G., and Pizzo, S. V. (2005) *J. Immunol.* **174,** 2092–2097
61. Reddy, R. K., Mao, C., Baumeister, P., Austin, R. C., Kaufman, R. J., and Lee, A. S. (2003) *J. Biol. Chem.* **278,** 20915–20924
62. Okazaki, Y., Ohno, H., Takase, K., Ochiai, T., and Saito, T. (2000) *J. Biol. Chem.* **275,** 35751–35758
63. Molins, B., Peña, E., Padro, T., Casani, L., Mendieta, C., and Badimon, L. (2010) *Arterioscler. Thromb. Vasc. Biol.* **30,** 1246–1252
64. Misra, U. K., Gonzalez-Gronow, M., Gawdi, G., Wang, F., and Pizzo, S. V. (2004) *Cell. Signal* **16,** 929–938
65. Triantafilou, K., Fradelizi, D., Wilson, K., and Triantafilou, M. (2002) *J. Virol.* **76,** 633–643
66. Triantafilou, M., Wilson, K. M., and Triantafilou, K. (2001) *Cytometry* **43,** 279–289
67. Zhang, Y., Deng, Y., Luther, T., Müller, M., Ziegler, R., Waldherr, R., Stern, D. M., and Nawroth, P. P. (1994) *J. Clin. Invest.* **94,** 1320–1327
68. Hembrough, T. A., Swartz, G. M., Papathanassiu, A., Vlasuk, G. P., Rote, W. E., Green, S. J., and Pribluda, V. S. (2003) *Cancer Res.* **63,** 2997–3000
69. Rak, J., Milsom, C., May, L., Klement, P., and Yu, J. (2006) *Semin. Thromb. Hemost.* **32,** 54–70